

Myocardial Injury Pattern at MRI in COVID-19 Vaccine–associated Myocarditis



Matteo Fronza, MD • Paaladinesh Thavendiranathan, MD, SM • Victor Chan, MD • Gauri Rani Karur, MD • Jacob A. Udell, MD, MPH • Rachel M. Wald, MD • Rachel Hong, BSc • Kate Hanneman, MD, MPH

From the Department of Medical Imaging (M.F., P.T., V.C., G.R.K., R.M.W., R.H., K.H.) and Division of Cardiology (P.T., J.A.U., R.M.W.), Toronto General Hospital, Peter Munk Cardiac Centre, University Health Network (UHN), University of Toronto, 585 University Ave, 1 PMB-298, Toronto, ON, Canada M5G 2N2; and Department of Medical Imaging (M.F., P.T., V.C., G.R.K., R.M.W.) and Cardiovascular Division (J.A.U.), Women's College Hospital, University of Toronto, Toronto, Canada. Received October 9, 2021; revision requested November 22; revision received December 29; accepted January 20, 2022. Address correspondence to K.H. (email: kate.hanneman@uhn.ca).

Supported by a grant from the Joint Division of Medical Imaging, Canadian Radiological Foundation (CRF), and the Canadian Heads of Academic Radiology (CHAR). P.T. supported by a Canada Research Chair in Cardio-oncology. J.A.U. supported by a Department of Medicine, University of Toronto Merit Award and an Ontario Ministry of Colleges and Universities Early Researcher Award (ER15-11-037).

Conflicts of interest are listed at the end of this article.

See also the editorial by Raman and Neubauer in this issue.

Radiology 2022; 304:553–562 • <https://doi.org/10.1148/radiol.212559> • Content codes:  

Background: There are limited data on the pattern and severity of myocardial injury in patients with COVID-19 vaccination–associated myocarditis.

Purpose: To describe myocardial injury following COVID-19 vaccination and to compare these findings to other causes of myocarditis.

Materials and Methods: In this retrospective cohort study, consecutive adult patients with myocarditis with at least one T1-based and at least one T2-based abnormality at cardiac MRI performed at a tertiary referral hospital from December 2019 to November 2021 were included. Patients were classified into one of three groups: myocarditis following COVID-19 vaccination, myocarditis following COVID-19 illness, and other myocarditis not associated with COVID-19 vaccination or illness.

Results: Of the 92 included patients, 21 (23%) had myocarditis following COVID-19 vaccination (mean age, 31 years \pm 14 [SD]; 17 men; messenger RNA–1273 in 12 [57%] and BNT162b2 in nine [43%]). Ten of 92 (11%) patients had myocarditis following COVID-19 illness (mean age, 51 years \pm 14; three men) and 61 of 92 (66%) patients had other myocarditis (mean age, 44 years \pm 18; 36 men). MRI findings in the 21 patients with vaccine-associated myocarditis included late gadolinium enhancement (LGE) in 17 patients (81%) and left ventricular dysfunction in six (29%). Compared with other causes of myocarditis, patients with vaccine-associated myocarditis had a higher left ventricular ejection fraction and less extensive LGE, even after controlling for age, sex, and time from symptom onset to MRI. The most frequent location of LGE in all groups was subepicardial at the basal inferolateral wall, although septal involvement was less common in vaccine-associated myocarditis. At short-term follow-up (median, 22 days [IQR, 7–48 days]), all patients with vaccine-associated myocarditis were asymptomatic with no adverse events.

Conclusion: Cardiac MRI demonstrated a similar pattern of myocardial injury in vaccine-associated myocarditis compared with other causes, although abnormalities were less severe, with less frequent septal involvement and no adverse events over the short-term follow-up.

© RSNA, 2022

Online supplemental material is available for this article.

Myocarditis is a nonischemic inflammatory disease of the myocardium that has diverse causes, clinical patterns, and outcomes (1). Characteristic features are inflammation and myocyte damage, which may be mediated both by direct invasion of the myocardium in the setting of viral infection and by the host's immune response (2). Acute myocarditis is more common in men compared with women, although the incidence is difficult to establish as the clinical presentation is often nonspecific and endomyocardial biopsy is not routinely performed (3).

Myocarditis following immunization is a rare event that has received increased attention recently due to reports of myocardial injury in a minority of patients after receiving messenger RNA (mRNA)–based COVID-19 vaccines (4,5). As of December 2021, more than 4.5 billion people worldwide had received a dose of a COVID-19 vaccine (6). Therefore, serious adverse events associated with

administration of vaccines targeting COVID-19 are highly relevant to the public, clinicians, and other policy makers, even if the incidence is rare. Importantly, COVID-19 illness can also result in myocardial injury, which is associated with adverse outcomes in hospitalized patients and should be balanced against the risk of vaccine-related complications (7,8).

Cardiac MRI has an important role in the assessment of acute myocarditis with unparalleled ability for noninvasive characterization of myocardial tissue (9). Several recent case series have described MRI findings in hospitalized patients with myocarditis following COVID-19 vaccination (10–12). However, there are limited data on the extent of myocardial injury in comparison to other causes of myocarditis, particularly in nonhospitalized patients. Understanding the pattern and extent of myocardial injury and its implications will allow for improved care of these

Abbreviations

LGE = late gadolinium enhancement, LVEF = left ventricular ejection fraction, mRNA = messenger RNA

Summary

The pattern of myocardial injury at MRI in patients after COVID-19 vaccination was similar to that of other causes of myocarditis, but with less severity.

Key Results

- In this retrospective study of 92 patients with myocarditis, cardiac MRI scans demonstrated a similar pattern of injury in 21 patients with myocarditis following COVID-19 vaccination compared with that of other causes, including subepicardial late gadolinium enhancement.
- Myocardial abnormalities were less severe in patients with vaccine-associated myocarditis (eg, less functional impairment, lower native T1, and less frequent involvement of the septum) compared with other forms of myocarditis.

patients and may help address vaccine hesitancy. The aim of this study was to determine the pattern and extent of MRI findings in myocarditis associated with COVID-19 vaccination and to compare these findings with other causes of myocarditis.

Materials and Methods

Study Design and Participants

This retrospective cohort study was approved by the institutional ethics committee, and the requirement for written informed consent was waived. Hospitalized or nonhospitalized consecutive adult patients (≥ 18 years of age) who were referred to a tertiary hospital network for evaluation of myocarditis with cardiac MRI from December 2019 to November 2021 were identified. Inclusion criteria were fulfillment of the clinical presentation and diagnostic testing criteria of the European Society of Cardiology for clinically suspected myocarditis (13) and both of the main revised Lake Louise criteria for nonischemic myocardial inflammation on MRI scans (at least one T1-based criteria and at least one T2-based criteria; additional details are provided in Appendix E1 [online]) (14). The exclusion criterion was MRI performed for follow-up of previously diagnosed myocarditis.

Demographic characteristics, vaccine administration, medications, blood test results, electrocardiographic parameters, and clinical outcomes data were extracted from the electronic patient record. Patients were classified into one of three groups: COVID-19 vaccine-associated myocarditis (symptom onset within 14 days of vaccine administration with no other cause of myocarditis identified), COVID-19 illness-associated myocarditis (symptom onset within 14 days of confirmed SARS-CoV-2 infection based on reverse transcriptase-polymerase chain reaction assays of nasopharyngeal swabs with no other cause of myocarditis identified), and other myocarditis (all other patients meeting the inclusion criteria without temporally associated COVID-19 vaccine administration or known COVID-19 illness) (15,16). Adverse cardiac events were evaluated at short-term follow-up, including death, arrhythmia (defined as sustained atrial or ventricular arrhythmia lasting at least 30 seconds), and heart failure hospitalization. Clinically available blood test

results were collected, including high-sensitivity cardiac troponin I, B-type natriuretic peptide, and C-reactive protein.

MRI Technique

Cardiac MRI studies were performed using 1.5-T or 3-T scanners (MAGNETOM Avanto^{fit} and Skyra^{fit}; Siemens Medical Solutions) with commercially available cardiac surface coils. The MRI protocol included long-axis and a stack of short-axis cine balanced steady-state free precession sections (8-mm section thickness and 2-mm intersection gap) and a stack of black-blood T2-weighted spectral attenuated inversion-recovery, or SPAIR, images at matching short-axis locations. Images with late gadolinium enhancement (LGE) were acquired using a two-dimensional, phase-sensitive inversion-recovery technique starting 12 minutes after administration of intravenous contrast material (0.15 mmol/kg body weight of gadobutrol; Bayer) (17). A single midventricular short-axis T1 and T2 mapping section was acquired using a modified Look-Locker inversion recovery, or MOLLI, technique for native T1 mapping, with a 5(3)3 inversion grouping, (18) and a matching T2 map using a T2 preparation technique with the read-out varying according to the external field strength (balanced steady-state free precession at 1.5-T MRI and fast low-angle shot, or FLASH, at 3-T MRI) (19). Pixel-based T1 and T2 maps were automatically generated with the scanner by using inline motion correction algorithms.

MRI Analysis

MRI studies were analyzed independently by two experienced fellowship-trained observers (M.F. and V.C., both with 2 years of cardiac imaging experience) who were blinded to all clinical information with commercially available tools (Circle cvi42; Circle Cardiovascular Imaging). Ventricular volume, function, and mass were measured using semiautomated contour detection with manual correction, if required, per established standards (20). Global longitudinal, circumferential, and radial strain (global longitudinal strain [three long-axis views], global radial strain, and global circumferential strain [entire short-axis stack], respectively) were calculated from balanced steady-state free precession images by using feature tracking strain analysis. The presence of LGE and regional T2-weighted hyperintensity was evaluated visually (present or not), globally, and according to the American Heart Association 17-segment model (21). For assessment of LGE, the predominant pattern was classified as subendocardial, midwall, subepicardial, or transmural. LGE was quantified using a signal-intensity threshold of 4 SDs above visually normal reference myocardium, expressed in grams and as a percentage of left ventricular mass. Source T1 and T2 mapping images were examined for artifacts, and any segments with an artifact were excluded from analysis. Septal T1 and T2 relaxation times were assessed by manually drawing a region of interest at the midinterventricular septum, avoiding the right ventricular insertion points and blood pool. Maximum T1 and T2 values were also measured by manually drawing a region of interest in areas of visually maximum myocardial values based on the color map, with a minimum region of interest size of 0.5 cm². Per current guidelines, abnormal maximum T1 and T2 values were defined as 2 SDs above the mean of sequence-specific local ref-

erence values (high T2 was defined as >52 msec at 1.5 T and >45 msec at 3 T; high T1 was defined as >1067 msec at 1.5 T and >1289 msec at 3 T) (22). To facilitate combined analysis of multiscanner data, T1 and T2 values were converted to a z score using scanner-specific local reference values (patient value minus mean of reference range divided by SD of reference range) (23). In this case, z scores provided an assessment of how many SDs each patient's T1 or T2 value was above or below the mean for the normal range for each scanner.

Statistical Analysis

Categorical data are presented as counts and percentages, and continuous variables are presented as means \pm SDs and medians with IQRs. All continuous data were tested for normal distribution using the Shapiro-Wilk test. Comparisons between groups were conducted using one-way analysis of variance for continuous variables with normal distribution and the Kruskal-Wallis test for continuous variables with nonnormal distribution, with post hoc tests for significance between groups using Bonferroni correction. The Fisher exact test was used to compare categorical variables. We performed sensitivity analyses, restricting the vaccine-associated group to those without a history of COVID-19 infection and restricting the other myocarditis group to those with a non-COVID-19 viral or postinfectious cause of myocarditis. Spearman correlation analysis was used to evaluate associations between continuous variables. Linear regression was used to evaluate the relationship between continuous MRI parameters and patient group, controlling for patient age, sex, and time from symptoms to MRI. All tests were two tailed and $P < .05$ was considered indicative of a statistically significant difference. Analysis was performed with Stata software (version 14.1, StataCorp) and data were visualized with Prism (version 9.0.2, GraphPad Software).

Results

Patient Characteristics

Ninety-six patients were evaluated for eligibility. Four patients were excluded because MRI was performed for follow-up of previously diagnosed myocarditis (Fig 1), leaving 92 patients (mean age, 41 years \pm 18; 56 men) (Table 1). Twenty-one of 92 patients (23%) had COVID-19 vaccine-associated myocarditis, for whom the mean age was 31 years \pm 14; 17 (81%) were male. Of the 92 patients, 10 (11%) had myocardial injury following COVID-19 illness and 61 (66%) had myocarditis not temporally associated with either COVID-19 vaccination or illness (myocarditis was non-COVID-19 viral or postinfectious in 19 patients [31%], autoimmune in eight patients [13%], drug-related in six patients [10%], hyper-eosinophilic in three patients [5%], and other or unknown in 25 patients [41%]). Patients with vaccine-associated myocarditis were younger and more frequently male compared with the other groups. The median time from symptom onset to MRI was 11 days (IQR, 4–29 days).

COVID-19 Vaccine-associated Myocarditis

Among the 21 patients with vaccine-associated myocarditis, symptom onset followed administration of mRNA-1273 (Mod-

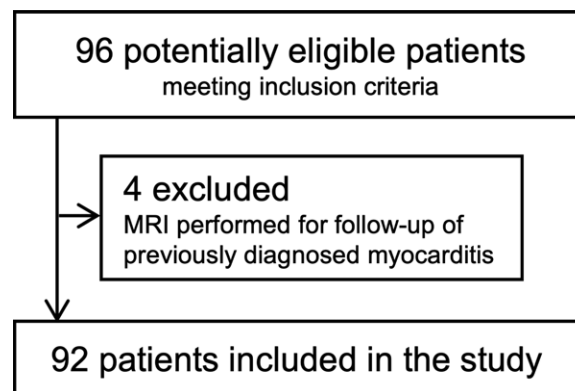


Figure 1: Flowchart of patient selection.

erna) in 12 (57%) and BNT162b2 (Pfizer–BioNTech) in nine (43%) and occurred after administration of the second vaccine dose of a two-dose series in 17 (81%). In those who received two doses, the median interval between the first and second dose was 33 days (IQR, 25–41 days). Two patients had a history of COVID-19 illness, both of whom had mild disease severity and recovered at home, with an interval between COVID-19 diagnosis and vaccine administration of 111 days and 155 days. Chest pain occurred in all 21 patients and started at a median of 3 days (IQR, 1–7 days) after vaccination, lasting 1–6 days. Fourteen (67%) of the 21 patients were admitted to the hospital, with a median length of stay of 3 days (IQR, 2–5 days). No patients were admitted to the intensive care unit. Of the 21 patients, 10 (48%) were treated with colchicine, seven (33%) with aspirin, four (20%) with ibuprofen, and one (5%) with steroids. Troponin levels were elevated in all patients admitted to the hospital (>26 pg/mL) and substantially decreased by the time of discharge (median, 2723 pg/mL [IQR, 1500–5772 pg/mL] vs 49 pg/mL [IQR, 0–205 pg/mL]; $P = .001$).

Cardiac MRI of Patients with Vaccine-associated Myocarditis

MRI characteristics are provided in Table 2. Abnormal MRI findings among the patients with myocarditis following COVID-19 vaccination included LGE in 17 of 21 (81%), high T1 in 14 of 21 (67%), high T2 in 16 of 21 (76%), hyperintense signal on T2-weighted images in 15 of 19 (79%), and systolic left ventricular dysfunction (left ventricular ejection fraction [LVEF] $<55\%$) in six of 21 (29%) (Fig 2). In all patients with myocarditis after vaccination ($n = 21$), at least one T2-based abnormality colocalized within the same myocardial segment as a T1-based abnormality, including LGE. None of the MRI parameters differed significantly between vaccine types.

The peak high-sensitivity cardiac troponin I level correlated significantly with the maximum native T2 z score ($r = 0.50$, $P = .040$), LVEF ($r = -0.58$, $P = .015$), global circumferential strain ($r = 0.66$, $P = .005$), and global radial strain ($r = -0.59$, $P = .013$) but not with the maximum native T1 z score, LGE extent, or global longitudinal strain.

Comparison of COVID-19 and Other Causes of Myocarditis

Compared with patients with other causes of myocarditis, patients with vaccine-associated myocarditis had a significantly

Table 1: Patient Characteristics and Blood Test Results

Characteristic	All Patients (n = 92)	COVID-19 Vaccine Group (n = 21)	COVID-19 Illness Group (n = 10)	Other Myocarditis Group (n = 61)	P Value
Age (y)*	41 ± 18	31 ± 14	51 ± 14 [†]	44 ± 18 [†]	.002
Sex					
M	56 (61)	17 (81)	3 (30) [†]	36 (59)	.026
F	36 (39)	4 (19)	7 (70)	25 (41)	
Height (cm)*	170 ± 17	172 ± 23	169 ± 10	170 ± 18	.88
Weight (kg)*	78 ± 23	79 ± 15	81 ± 17	78 ± 27	.91
Body surface area (m ²)*	1.9 ± 0.3	2.0 ± 0.2	1.9 ± 0.2	1.9 ± 0.3	.37
Comorbidities [‡]					
Diabetes	8 (10)	0 (0)	0 (0)	8 (16)	.10
Hypertension	14 (18)	0 (0)	2 (33) [†]	12 (24) [†]	.02
Dyslipidemia	10 (13)	0 (0)	1 (17)	9 (18)	.08
Smoking	7 (9)	1 (5)	0 (0)	6 (12)	.81
Hospital admission	61 (66)	14 (67)	4 (40)	43 (70)	.15
Symptoms at presentation [§]					
Palpitations	12 (14)	4 (19)	1 (10)	7 (13)	.81
Chest pain	71 (83)	21 (100)	9 (90)	41 (75) [†]	.02
Shortness of breath	28 (33)	2 (10)	5 (50) [†]	21 (38) [†]	.02
Blood tests (pg/mL)					
Peak hsTnI	3017 (363–7272)	2000 (856–5477)	3550 (222–6877)	3048 (349–7664)	.98
Peak CRP	27 (2–86)	14 (2–38)	26 (17–580)	34 (0–115)	.45
Peak BNP	3 (0–722)	0 (0–3)	0 (0–0)	196 (0–915) [†]	.04
ECG findings**					
PR interval (msec) [#]	159 (141–171)	162 (156–170)	152 (148–172)	153 (136–171)	.48
QRS duration (msec) [#]	88 (80–100)	94 (82–100)	88 (68–102)	88 (80–98)	.82
QT interval (msec) [#]	388 (350–420)	394 (368–416)	352 (348–398)	388 (346–426)	.57
ST-segment changes	23 (37)	6 (40)	1 (25)	16 (37)	.99

Note.—Except where indicated, data are numbers of patients, with percentages in parentheses. *P* values for the three-group comparison were derived using one-way analysis of variance and the Kruskal-Wallis test or Fisher exact test, as appropriate for the type of data. BNP = B-type natriuretic peptide, CRP = C-reactive protein, ECG = electrocardiography, hsTnI = high-sensitivity troponin I.

* Data are means ± SDs.

[†] Post hoc test for comparison with COVID-19 vaccine group; statistically significant at *P* < .05.

[‡] Data were available in 78 patients (21 with vaccine-associated myocarditis, six with COVID-19 illness, and 51 with other myocarditis).

[§] Data were available in 86 patients (21 with vaccine-associated myocarditis, 10 with COVID-19 illness, and 55 with other myocarditis).

^{||} Data were available in 73 patients (17 with vaccine-associated myocarditis, four with COVID-19 illness, and 52 with other myocarditis).

[#] Data are medians, with IQRs in parentheses.

** Data were available in 62 patients (15 with vaccine-associated myocarditis, four with COVID-19 illness, and 43 with other myocarditis).

higher LVEF and right ventricular ejection fraction; less impaired global longitudinal strain, global circumferential strain, and global radial strain; lower native T1; and less extensive LGE (Fig 3, Table 2). Differences in the LVEF, global longitudinal strain, global circumferential strain, global radial strain, native T1, and LGE extent remained significant even after controlling for patient age, sex, and time from symptom onset to imaging (Table 3). Compared with patients with COVID-19 illness, patients with vaccine-associated myocarditis had a higher LVEF, less regional wall motion abnormalities, and lower native T1. Differences in LVEF remained significant even in the multivariable model. In all three patient groups, the most frequent pattern of LGE was subepicardial and the most frequent myocardial segment involved was the basal inferolateral wall (Fig 4). However, patients with COVID-19 illness and other myocarditis had a higher prevalence of abnormalities involving the basal to mid

anterior and inferior septum, while patients with vaccine-associated myocarditis rarely had abnormalities involving the anterior wall or septum. There were no significant differences in blood biomarkers or electrocardiographic parameters between groups.

Sensitivity Analysis

Conclusions of our primary analyses were unchanged when we excluded the two patients who had vaccine-associated myocarditis with a history of COVID-19 illness (Table E1 [online]), and when the other myocarditis group was restricted to patients with non-COVID-19 viral or postinfectious myocarditis (Table E2 [online]).

Follow-up

All patients with vaccine-associated myocarditis had short-term clinical follow-up for a median of 22 days (IQR, 7–48 days).

Table 2: Cardiac MRI Findings

Parameter	All Patients (n = 92)	COVID-10 Vaccine Group (n = 21)	COVID-19 Illness Group (n = 10)	Other Myocarditis Group (n = 61)	P Value
Left ventricle					
LVEDVI (mL/m ²)	85 (71–97)	79 (69–87)	81 (72–98)	88 (71–97)	.26
LVESVI (mL/m ²)	40 (32–49)	35 (29–40)	36 (31–47)	43 (34–55)*	.006
LVMI (g/m ²)	59 (47–68)	51 (46–61)	48 (40–59)	62 (50–76)*	.01
LVEF (%)	52 (46–57)	58 (53–59)	55 (49–57)*	50 (41–54)*	<.001
GLS (%)	−14 (−17 to −11)	−16 (−19 to −14)	−17 (−17 to −15)	−13 (−15 to −10)*	<.001
GCS (%)	−15 (−17 to −12)	−16 (−19 to −15)	−17 (−18 to −15)	−14 (−16 to −10)*	<.001
GRS (%)	23 (17–28)	26 (22–31)	28 (23–30)	21 (14–25)*	<.001
Low LVEF [†]	58 (63)	6 (29)	5 (50)	47 (77)*	<.001
Regional wall motion abnormality [†]	30 (33)	0 (0)	4 (40)*	26 (43)*	<.001
Right ventricle					
RVEDVI (mL/m ²)	82 (70–97)	84 (71–100)	82 (70–95)	82 (69–96)	.95
RVESVI (mL/m ²)	40 (31–48)	38 (32–46)	35 (28–44)	42 (31–50)	.46
RVEF (%)	51 (47–55)	54 (51–54)	55 (53–59)	51 (45–55)*	.02
Left atrial area (cm ²)	22 (19–26)	20 (16–22)	24 (22–28)	22 (19–27)	.04
Right atrial area (cm ²)	19 (15–22)	20 (13–21)	21 (17–24)	18 (15–21)	.21
Tissue characterization					
LGE presence [†]	85 (92)	17 (81)	9 (90)	59 (97)*	.06
Subendocardial LGE [†]	0 (0)	0 (0)	0 (0)	0 (0)	.99
Midwall LGE [†]	33 (36)	4 (19)	5 (50)	24 (39)	.13
Subepicardial LGE [†]	51 (55)	13 (62)	4 (40)	34 (56)	.56
Transmural LGE [†]	1 (1)	0 (0)	0 (0)	1 (2)	.99
LGE extent (%)	2 (1–5)	1 (0–2)	2 (1–2)	3 (1–6)*	.003
LGE extent (g)	3 (1–6)	1 (0–3)	2 (1–4)	4 (1–8)*	.002
LGE (no. of segments)	3 (1–5)	2 (1–3)	3 (1–4)	3 (1–6)*	.04
Hyperintense T2-weighted signal ^{††}	67 (77)	15 (79)	6 (75)	46 (77)	.99
Septal T2 z score [§]	0.6 (−0.5 to 1.8)	−0.3 (−0.7 to 1.5)	0.9 (−0.1 to 1.3)	0.9 (−0.1 to 2.0)	.13
Maximum T2 z score [§]	2.7 (1.6–3.8)	2.7 (2.2–3.1)	2.7 (1.6–3.2)	3.1 (1.5–4.4)	.37
High T2 ^{†§}	61 (69)	16 (76)	7 (70)	38 (66)	.70
Septal native T1 z score	1.4 (0.2–3.1)	0.4 (−0.2 to 0.6)	1.5 (0.8–2.4)*	2.2 (0.7–4.1)*	<.001
Maximum native T1 z score	3.7 (2.3–5.7)	2.3 (0.6–3.1)	4.0 (2.9–4.7)*	4.3 (2.8–7.2)*	<.001
High native T1	71 (81)	14 (67)	9 (90)	48 (84)	.20
Pericardium[†]					
Pericardial enhancement	39 (42)	9 (43)	3 (30)	27 (44)	.77
Pericardial edema	35 (38)	4 (19)	3 (30)	28 (46)	.07
Pericardial effusion	33 (36)	4 (19)	1 (10)	28 (46)	.02
Time from symptom onset to MRI (d)	11 (4–29)	13 (5–61)	45 (13–95)	7 (3–20)	.001

Note.—Except where indicated, data are medians with IQRs in parentheses. *P* values for the three-group comparison were derived using one-way analysis of variance and the Kruskal-Wallis test or Fisher exact test, as appropriate for the type of data. GCS = global circumferential strain, GLS = global longitudinal strain, GRS = global radial strain, LGE = late gadolinium enhancement, LVEDVI = left ventricular end-diastolic volume indexed to body surface area, LVEF = left ventricular ejection fraction, LVESVI = left ventricular end-systolic volume indexed to body surface area, LVMI = left ventricular mass index, RVEDVI = right ventricular end-diastolic volume indexed to body surface area, RVEF = right ventricular ejection fraction, RVESVI = right ventricular end-systolic volume indexed to body surface area.

* Post hoc test for comparison with the COVID-19 vaccine group; statistically significant at *P* < .05.

[†] Data are numbers of patients, with percentages in parentheses.

[‡] Data were available in 87 patients (19 with vaccine-associated myocarditis, eight with COVID-19 illness, and 60 with other myocarditis).

[§] Data were available in 89 patients (21 with vaccine-associated myocarditis, 10 with COVID-19 illness, and 58 with other myocarditis).

^{||} Data were available in 88 patients (21 with vaccine-associated myocarditis, 10 with COVID-19 illness, and 57 with other myocarditis).

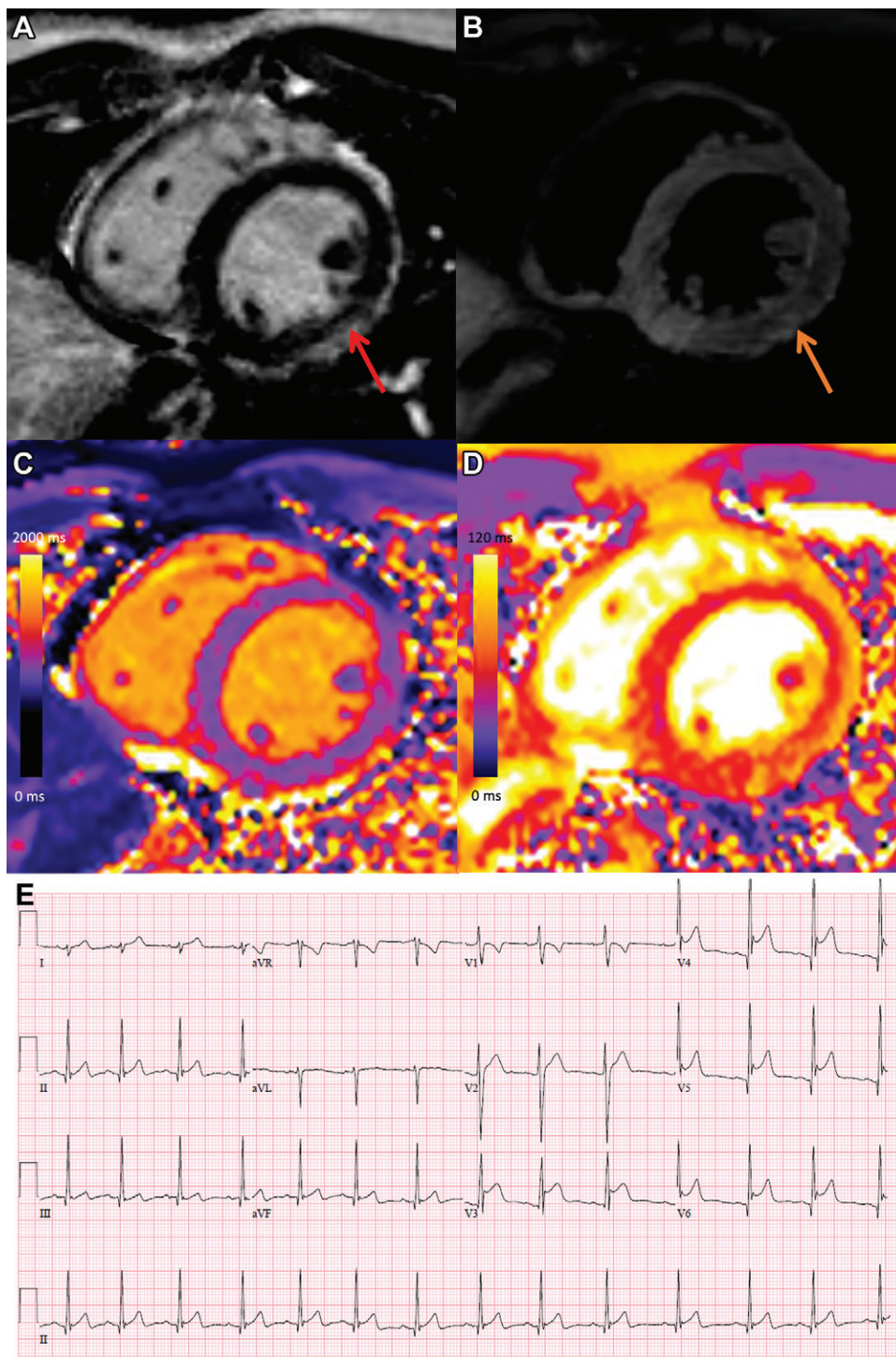


Figure 2: COVID-19 vaccine–associated myocarditis. Short-axis 1.5-T MRI scans and electrocardiographic findings in a 19-year-old man with myopericarditis who presented with chest pain 3 days following the second dose of messenger RNA–1273 COVID-19 vaccine. **(A)** Cardiac MRI late gadolinium enhanced scan obtained 2 days after symptom onset demonstrates midwall to subepicardial late gadolinium enhancement at the basal to mid-inferior lateral wall with adjacent pericardial enhancement (arrow). **(B)** T2-weighted MRI scan shows corresponding hyperintensity (arrow). **(C, D)** Parametric maps show abnormal high native T1 (C, 1095 msec, maximum region of interest) and abnormal high native T2 (D, 57 msec, maximum region of interest). **(E)** Electrocardiogram demonstrates diffuse concave upward ST-segment elevation except in leads aVR and V₁, upright T waves in the leads with ST-segment elevation, and PR depression consistent with pericarditis. The peak high-sensitivity troponin I level was 5772 pg/mL. The patient was admitted to the hospital and discharged after 2 days following complete resolution of symptoms and was asymptomatic with normal troponin levels at short-term follow-up.

At follow-up, all 21 patients (100%) were asymptomatic; eight of 21 (38%) had normal troponin levels, nine of 21 (43%) had reduced but still mildly elevated troponin levels, and four of 21 did not have follow-up troponin levels available. Of the six patients with impaired LVEF at MRI, four underwent subsequent transthoracic echocardiography or follow-up MRI, which demonstrated normal LVEFs in all. No patient with vaccine-associated myocarditis had an adverse cardiac event over the short-term follow-up.

Among the 71 patients with COVID-19 illness and other myocarditis, seven and 42 had clinical follow-up for a median of 211 days (IQR, 94–295 days) and 195 days (IQR, 87–415 days), respectively. The COVID-19 illness group included three major adverse cardiovascular events (one hospitalization for heart failure and two arrhythmia events [one patient subsequently underwent placement of an implantable cardioverter-defibrillator]), while the other myocarditis group included five major adverse cardiovascular events (two hospitalizations for heart failure and three arrhythmia events [four patients subsequently underwent placement of an implantable cardioverter-defibrillator]). There were no deaths in any group. As expected, the follow-up duration for the other two groups was much longer than that for the vaccine group, given the relatively short amount of time that COVID-19 vaccines had been administered.

Discussion

In this retrospective cohort study of 92 patients who met both clinical and imaging diagnostic criteria for acute myocarditis, we identified 21 patients with myocarditis following

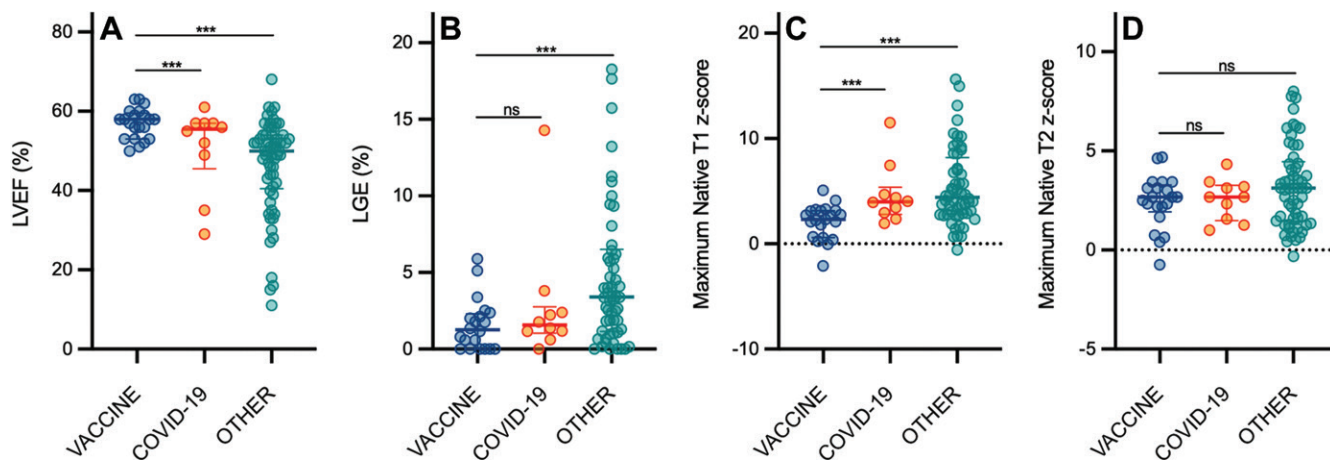


Figure 3: Scatterplots show (A) left ventricular ejection fraction (LVEF), (B) late gadolinium enhancement (LGE), (C) native T1, and (D) native T2 according to patient group. Graphs for MRI parameters depict individual patient data points with error bars displayed as medians and IQRs. There were significant differences in the maximum native T1 z score, maximum native T2 z score, and LGE extent (as a percentage of left ventricular mass) between patients with vaccine-associated myocarditis (vaccine) and those with other myocarditis (other). All other comparisons between patients with vaccine-associated myocarditis and patients with COVID-19 illness (COVID-19) or other myocarditis were not significant (ns). *** = $P < .05$; statistically significant.

COVID-19 vaccine administration who were younger and more frequently male compared with 10 patients who had recovered from COVID-19 illness and 61 patients with other causes of myocarditis. To our knowledge, this is the first report of cardiac MRI findings in both hospitalized and nonhospitalized patients with myocarditis following COVID-19 vaccination in comparison with patients with other causes of myocarditis, including COVID-19 illness. Abnormal MRI findings among patients with myocarditis following COVID-19 vaccination included late gadolinium enhancement (LGE) in 81%, high T1 in 67%, high T2 in 76%, and systolic left ventricular dysfunction in 29%. MRI revealed a similar pattern of myocardial injury in patients with myocarditis following COVID-19 vaccination compared with that of other causes, including subepicardial LGE and edema at the basal inferior lateral wall, although patient demographics differed and abnormalities were less severe. Patients with vaccine-associated myocarditis had higher left ventricular ejection fraction and lower native T1 values compared with those

Table 3: Univariable and Multivariable Linear Regression Parameters with Vaccine-associated Myocarditis as the Reference Group

Parameter	COVID-19 Illness		Other Myocarditis	
	β coefficient*	<i>P</i> Value	β coefficient†	<i>P</i> Value
Univariable models				
LVEF (%)	-6.1 (-11.3, -0.9)	.024	-5.3 (-7.9, -2.6)	<.001
GLS (%)	1.1 (-1.6, 3.9)	.41	1.9 (0.9, 3.0)	.001
GCS (%)	1.3 (-1.0, 3.7)	.26	2.0 (1.0, 2.9)	<.001
GRS (%)	-2.2 (-7.4, 2.9)	.38	-3.6 (-5.5, -1.8)	<.001
Maximum T1 z score	2.6 (1.0, 4.2)	.003	1.7 (0.7, 2.9)	.002
Maximum T2 z score	0.1 (-0.9, 1.1)	.79	0.5 (-0.1, 1.1)	.12
LGE extent, no. of segments	1.1 (-0.5, 2.7)	.19	1.2 (0.3, 2.1)	.012
Multivariable models‡				
LVEF (%)	-8.8 (-15.6, -2.1)	.013	-5.7 (-8.5, -3.0)	<.001
GLS (%)	2.4 (-1.6, 6.4)	.23	1.8 (0.7, 2.9)	.002
GCS (%)	2.7 (-0.2, 5.6)	.07	2.4 (1.4, 3.3)	<.001
GRS (%)	-6.2 (-12.4, -0.5)	.048	-4.6 (-6.5, -2.7)	<.001
Maximum T1 z score	1.4 (-0.7, 3.4)	.18	1.2 (0.3, 2.4)	.044
Maximum T2 z score	0.5 (-0.9, 1.9)	.48	0.4 (-0.3, 1.0)	.25
LGE extent (no. of segments)	1.4 (-1.0, 3.6)	.24	1.4 (0.3, 2.5)	.011

Note.—Data in parentheses are 95% CIs. Linear regression was used to evaluate the relationship between continuous MRI parameters and the patient group in univariable and multivariable models controlling for patient age, sex, and time from symptom onset to MRI. GCS = global circumferential strain, GLS = global longitudinal strain, GRS = global radial strain, LGE = late gadolinium enhancement, LVEF = left ventricular ejection fraction.

* Average difference in the magnitude of each MRI parameter (dependent variable) between COVID-19 illness-associated myocarditis and COVID-19 vaccination-associated myocarditis (independent variable; vaccine-associated myocarditis is the reference group).

† Average difference in the magnitude of each MRI parameter (dependent variable) between other causes of myocarditis and COVID-19 vaccination-associated myocarditis (independent variable; vaccine-associated myocarditis is the reference group).

‡ Individual multivariable linear regression models for each MRI parameter (as the dependent variable) and disease group (as the independent variable) were adjusted for patient age, sex, and time from symptom onset to MRI.

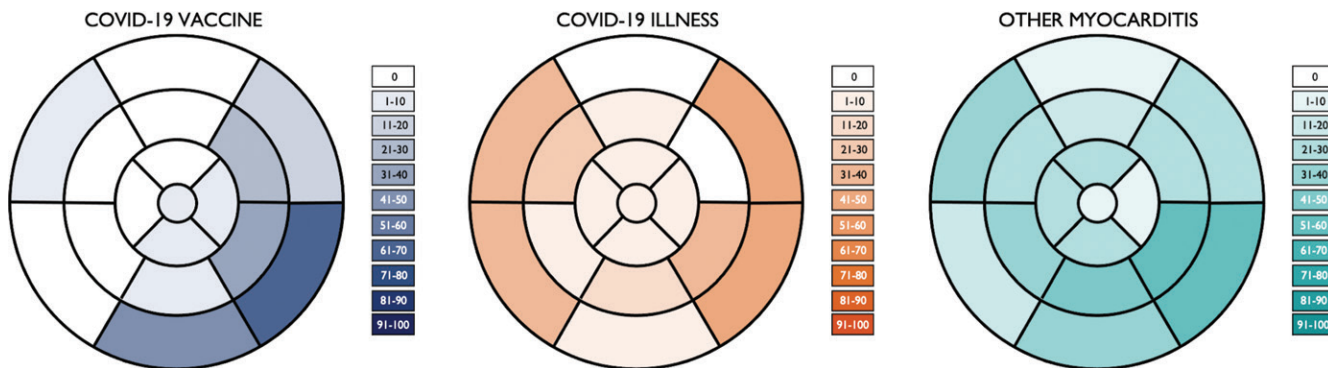


Figure 4: Segmental distribution of MRI abnormalities. Color-shaded bull's-eye plots represent the percentage of patients in each group with late gadolinium enhancement and/or hyperintensity on T2-weighted images for each myocardial segment according to a standardized 17-segment model. COVID-19 vaccine = patients with vaccine-associated myocarditis, COVID-19 illness = patients with myocarditis who had recovered from COVID-19, other myocarditis = patients with other causes of myocarditis.

with COVID-19 illness and other causes of myocarditis, and they demonstrated rapid clinical improvement with no adverse events over short-term follow-up.

Our observations are concordant with case series of hospitalized patients reporting that most patients with vaccine-associated myocarditis were younger men presenting after the second vaccine dose, with frequent presence of LGE and myocardial edema on MRI scans and rapid improvement in clinical symptoms at short-term follow-up (10,11,24). Other MRI findings in our cohort included high T1 and T2 mapping values and impaired myocardial strain. T1 and T2 mapping are quantitative tissue characterization techniques that provide complementary information, particularly in the setting of myocardial inflammation. High T2 is specific for increased tissue water and can help discriminate between active and healed myocarditis (25). Native T1 is also elevated in the setting of edema, although unlike T2, this change is not specific for acute inflammation and can alternatively reflect fibrosis or infiltration. This might account for the significant correlation between peak troponin level and native T2, but not with native T1, in our study.

Unlike prior reports, our findings demonstrate that myocardial injury was detectable in patients with acute myocarditis who did not require hospital admission and the severity of MRI abnormalities was milder, in general, compared with that of patients with other causes of myocarditis, even after controlling for age, sex, and time from symptom onset to imaging. Patients with myocarditis following COVID-19 illness had a lower LVEF, higher prevalence of regional left ventricular dysfunction, and higher native T1 compared with those with vaccine-associated myocarditis, although other MRI parameters did not differ significantly. This suggests that the imaging phenotype of patients with COVID-19-related myocardial injury may be intermediate between vaccine-associated myocarditis and other causes.

Presentation after the second vaccine dose or after the first dose in the context of prior SARS-CoV-2 infection in most patients indicates that prior exposure is relevant and necessitates continued surveillance for postvaccination myocarditis, particularly following booster doses. Although non-mRNA vaccines were also administered in Canada, all patients with vaccine-associated myocarditis in our cohort presented after receiving an mRNA-based COVID-19 vaccine. The mechanisms by which a

host's immunologic response to mRNA-based COVID-19 vaccination could lead to myocarditis in a small minority of patients warrants further study, particularly because other mRNA-based vaccines and therapies are in development (26,27).

Milder MRI abnormalities in patients with vaccine-associated myocarditis compared with other causes raises the possibility that this group may have a lower future adverse event rate. Lack of any adverse events in our patients with vaccine-associated myocarditis over short-term follow-up is reassuring. However, longer-term follow-up is needed, particularly given the association of LGE with adverse cardiac events in nonvaccine-associated myocarditis (28,29). Interestingly, one prior study found that patchy and midwall, but not subepicardial, patterns of LGE were associated with adverse events in patients with nonvaccine-associated myocarditis (30). Similarly, a septal but not lateral LGE location was associated with major adverse cardiac events (30). This requires further investigation given that the majority of patients with vaccine-associated myocarditis in our study had a subepicardial pattern of LGE with a predilection for the basal to mid-lateral wall and infrequent involvement of the septum, which may be associated with relatively favorable outcomes. LGE usually reflects fibrosis in ischemic and nonischemic cardiomyopathies; however, in patients with acute myocarditis it often reflects an increased volume of distribution of the gadolinium-based contrast agent in the affected region related to myocyte necrosis and edema. In all patients with vaccine-associated myocarditis, LGE colocalized with edema in at least one segment, which is associated with better prognosis compared with isolated LGE without T2 hyperintensity and confers the possibility of recovery as edema improves with time (31).

Our study has limitations, including a modest sample size and a short follow-up for patients with myocarditis following vaccination. More than one MRI scanner was used for imaging, which impacts quantitative parametric mapping. To address this, we interpreted mapping values in the context of scanner-specific local reference ranges and calculated z scores for T1 and T2 values. The timing of MRI after symptom onset varied, which could impact detection of myocardial edema as MRI markers of edema typically demonstrate rapid improvement during the first few weeks after symptom onset (32). There were also significant differences in patient age and sex between groups. Although

we adjusted for age, sex, and timing of imaging in our analysis, it is possible that this did not fully account for differences between groups. Only midventricular T1 and T2 mapping sections were examined, which could underestimate maximum T1 and T2 values if regional disease was only present in other areas of the myocardium. However, LGE and T2-weighted imaging were performed with coverage of the entire myocardium from base to apex. This may account for the overall slightly higher prevalence of abnormalities on LGE and T2-weighted images compared with T1 and T2 mapping, respectively. As this was not a population-based study, we could not calculate the incidence of vaccine-associated myocarditis. There is no standardized definition of vaccine-associated myocarditis or COVID-19–related myocardial injury in the literature to date, particularly with respect to the timing of symptom onset after vaccine administration or COVID-19 diagnosis. For consistency, we used the same 14-day interval between vaccination or COVID-19 diagnosis to symptom onset to define both groups. Finally, histologic confirmation of myocarditis was not available as endomyocardial biopsy is not frequently performed at our center unless there is clinical evidence that the results will have a meaningful effect on therapeutic decisions (33). Our findings should be confirmed in future large, multicenter studies with longer-term follow-up.

In conclusion, our study results demonstrate that the pattern of MRI abnormalities in COVID-19 vaccine–associated myocarditis was similar to that of other causes, although patient demographics differed and MRI findings tended to be less severe. Overall, our study findings are generally consistent with an imaging phenotype that has good prognosis; however, further studies are needed to examine the long-term effects of mRNA-based COVID-19 vaccination on the heart, to determine the risk associated with booster doses, and to inform recommendations for vaccination in patients with a history of myocarditis.

Author contributions: Guarantors of integrity of entire study, **M.F., K.H.**; study concepts/study design or data acquisition or data analysis/interpretation, all authors; manuscript drafting or manuscript revision for important intellectual content, all authors; approval of final version of submitted manuscript, all authors; agrees to ensure any questions related to the work are appropriately resolved, all authors; literature research, **M.F., K.H.**; clinical studies, **M.F., V.C., R.H., K.H.**; experimental studies, **M.F.**; statistical analysis, **M.F., P.T., K.H.**; and manuscript editing, **M.F., P.T., V.C., G.R.K., J.A.U., R.M.W., K.H.**

Disclosures of conflicts of interest: **M.F.** No relevant relationships. **P.T.** No relevant relationships. **V.C.** No relevant relationships. **G.R.K.** No relevant relationships. **J.A.U.** Grants from Amgen, AstraZeneca, Bayer, Boehringer Ingelheim, Janssen, Novartis, Sanofi; consultant, Boehringer Ingelheim, Novartis, Sanofi; honoraria from GlaxoSmithKline and Sanofi. **R.M.W.** No relevant relationships. **R.H.** No relevant relationships. **K.H.** Honoraria from Sanofi Genzyme, Amicus, and Medscape.

References

- Sanchez Tijmes F, Thavendiranathan P, Udell JA, Seidman MA, Hanneman K. Cardiac MRI Assessment of Nonischemic Myocardial Inflammation: State of the Art Review and Update on Myocarditis Associated with COVID-19 Vaccination. *Radiol Cardiothorac Imaging* 2021;3(6):e210252.
- Aretz HT, Billingham ME, Edwards WD, et al. Myocarditis. A histopathologic definition and classification. *Am J Cardiovasc Pathol* 1987;1(1):3–14.
- Ammirati E, Cipriani M, Moro C, et al. Clinical Presentation and Outcome in a Contemporary Cohort of Patients With Acute Myocarditis: Multicenter Lombardy Registry. *Circulation* 2018;138(11):1088–1099.
- Su JR, McNeil MM, Welsh KJ, et al. Myopericarditis after vaccination, Vaccine Adverse Event Reporting System (VAERS), 1990–2018. *Vaccine* 2021;39(5):839–845.
- Luk A, Clarke B, Dahdah N, et al. Myocarditis and Pericarditis After COVID-19 mRNA Vaccination: Practical Considerations for Care Providers. *Can J Cardiol* 2021;37(10):1629–1634.
- Holder J. The New York Times Tracking Coronavirus Vaccinations Around the World. <https://www.nytimes.com/interactive/2021/world/covid-vaccinations-tracker.html>. Published Jan. 29, 2021. Accessed December 15, 2021.
- Giustino G, Croft LB, Stefanini GG, et al. Characterization of Myocardial Injury in Patients With COVID-19. *J Am Coll Cardiol* 2020;76(18):2043–2055.
- Guo T, Fan Y, Chen M, et al. Cardiovascular Implications of Fatal Outcomes of Patients With Coronavirus Disease 2019 (COVID-19). *JAMA Cardiol* 2020;5(7):811–818.
- Pan JA, Lee YJ, Salerno M. Diagnostic Performance of Extracellular Volume, Native T1, and T2 Mapping Versus Lake Louise Criteria by Cardiac Magnetic Resonance for Detection of Acute Myocarditis: A Meta-Analysis. *Circ Cardiovasc Imaging* 2018;11(7):e007598.
- Kim HW, Jenista ER, Wendell DC, et al. Patients With Acute Myocarditis Following mRNA COVID-19 Vaccination. *JAMA Cardiol* 2021;6(10):1196–1201.
- Montgomery J, Ryan M, Engler R, et al. Myocarditis Following Immunization With mRNA COVID-19 Vaccines in Members of the US Military. *JAMA Cardiol* 2021;6(10):1202–1206.
- Starekova J, Bluemke DA, Bradham WS, Grist TM, Schiebler ML, Reeder SB. Myocarditis Associated with mRNA COVID-19 Vaccination. *Radiology* 2021;301(2):E409–E411.
- Caforio ALP, Pankuweit S, Arbustini E, et al. Current state of knowledge on aetiology, diagnosis, management, and therapy of myocarditis: a position statement of the European Society of Cardiology Working Group on Myocardial and Pericardial Diseases. *Eur Heart J* 2013;34(33):2636–2648, 2648a–2648d.
- Ferreira VM, Schulz-Menger J, Holmvang G, et al. Cardiovascular Magnetic Resonance in Nonischemic Myocardial Inflammation: Expert Recommendations. *J Am Coll Cardiol* 2018;72(24):3158–3176.
- Jain SS, Steele JM, Fonseca B, et al. COVID-19 Vaccination-Associated Myocarditis in Adolescents. *Pediatrics* 2021;148(5):e2021053427.
- Voinsky I, Baristaite G, Gurwitz D. Effects of age and sex on recovery from COVID-19: Analysis of 5769 Israeli patients. *J Infect* 2020;81(2):e102–e103.
- Kellman P, Arai AE. Cardiac imaging techniques for physicians: late enhancement. *J Magn Reson Imaging* 2012;36(3):529–542.
- Kellman P, Arai AE, Xue H. T1 and extracellular volume mapping in the heart: estimation of error maps and the influence of noise on precision. *J Cardiovasc Magn Reson* 2013;15(1):56.
- Wassmuth R, Prothmann M, Utz W, et al. Variability and homogeneity of cardiovascular magnetic resonance myocardial T2-mapping in volunteers compared to patients with edema. *J Cardiovasc Magn Reson* 2013;15(1):27.
- Schulz-Menger J, Bluemke DA, Bremerich J, et al. Standardized image interpretation and post-processing in cardiovascular magnetic resonance - 2020 update : Society for Cardiovascular Magnetic Resonance (SCMR): Board of Trustees Task Force on Standardized Post-Processing. *J Cardiovasc Magn Reson* 2020;22(1):19.
- Cerqueira MD, Weissman NJ, Dilsizian V, et al. Standardized myocardial segmentation and nomenclature for tomographic imaging of the heart. A statement for healthcare professionals from the Cardiac Imaging Committee of the Council on Clinical Cardiology of the American Heart Association. *Circulation* 2002;105(4):539–542.
- Messroghli DR, Moon JC, Ferreira VM, et al. Clinical recommendations for cardiovascular magnetic resonance mapping of T1, T2, T2* and extracellular volume: A consensus statement by the Society for Cardiovascular Magnetic Resonance (SCMR) endorsed by the European Association for Cardiovascular Imaging (EACVI). *J Cardiovasc Magn Reson* 2017;19(1):75 [Published correction appears in *J Cardiovasc Magn Reson* 2018;20(1):9].
- Thavendiranathan P, Zhang L, Zafar A, et al. Myocardial T1 and T2 Mapping by Magnetic Resonance in Patients With Immune Checkpoint Inhibitor-Associated Myocarditis. *J Am Coll Cardiol* 2021;77(12):1503–1516.
- Dionne A, Sperotto F, Chamberlain S, et al. Association of Myocarditis With BNT162b2 Messenger RNA COVID-19 Vaccine in a Case Series of Children. *JAMA Cardiol* 2021;6(12):1446–1450.
- Galán-Arriola C, Lobo M, Vilchez-Tschischke JP, et al. Serial Magnetic Resonance Imaging to Identify Early Stages of Anthracycline-Induced Cardiotoxicity. *J Am Coll Cardiol* 2019;73(7):779–791.
- Miao L, Zhang Y, Huang L. mRNA vaccine for cancer immunotherapy. *Mol Cancer* 2021;20(1):41.
- Pardi N, Hogan MJ, Porter FW, Weissman D. mRNA vaccines - a new era in vaccinology. *Nat Rev Drug Discov* 2018;17(4):261–279.

28. Grün S, Schumm J, Greulich S, et al. Long-term follow-up of biopsy-proven viral myocarditis: predictors of mortality and incomplete recovery. *J Am Coll Cardiol* 2012;59(18):1604–1615.
29. Yang F, Wang J, Li W, et al. The prognostic value of late gadolinium enhancement in myocarditis and clinically suspected myocarditis: systematic review and meta-analysis. *Eur Radiol* 2020;30(5):2616–2626.
30. Gräni C, Eichhorn C, Bière L, et al. Prognostic Value of Cardiac Magnetic Resonance Tissue Characterization in Risk Stratifying Patients With Suspected Myocarditis. *J Am Coll Cardiol* 2017;70(16):1964–1976 [Published correction appears in *J Am Coll Cardiol* 2017;70(21):2736.].
31. Aquaro GD, Ghebru Habtemicael Y, Camastra G, et al. Prognostic Value of Repeating Cardiac Magnetic Resonance in Patients With Acute Myocarditis. *J Am Coll Cardiol* 2019;74(20):2439–2448.
32. Luetkens JA, Homsí R, Dabir D, et al. Comprehensive Cardiac Magnetic Resonance for Short-Term Follow-Up in Acute Myocarditis. *J Am Heart Assoc* 2016;5(7):e003603.
33. Cooper LT, Baughman KL, Feldman AM, et al. The role of endomyocardial biopsy in the management of cardiovascular disease: a scientific statement from the American Heart Association, the American College of Cardiology, and the European Society of Cardiology. *J Am Coll Cardiol* 2007;50(19):1914–1931.